Journal of ELECTRONIC MATERIALS, Vol. 45, No. 8, 2016
DOI: 10.1007/s11664-016-4605-3

Alloying Effects on the Phase Stability and Mechanical Properties of Doped Cu-Sn IMCs: A First-Principle Study

YONG ZHANG,[1] DING-WANG YUAN,[1,2] JIANG-HUA CHEN,[1,4] GUANG ZENG,[3] TOU-WEN FAN,[1] ZI-RAN LIU,[1] CUI-LAN WU,[1] and LING-HONG LIU[1]

1.—Center for High Resolution Electron Microscopy, College of Materials Science and Engineering, Hunan University, Changsha 410082, China. 2.—Hunan Province Key Laboratory for Spray Deposition Technology and Application, Hunan University, Changsha 410082, China. 3.—Nihon Superior Centre for the Manufacture of Electronic Materials (NS CMEM), School of Mechanical and Mining Engineering, The University of Queensland, Brisbane, QLD 4072, Australia. 4.—e-mail: jhchen123@hnu.edu.cn

Cu-Sn phases are important intermetallic compounds formed at the interface between solder and substrate in the soldering process. They exist in several crystal structures (η', η, η_1 and η_2, etc.). The solid-state phase transformation that occurs among Cu-Sn intermetallic compounds is a crucial issue for industry applications, because the associated volume change inevitably leads to microstructural instability. Generally, four alloying elements, i.e., Ni, Au, Zn, and indium (In), are used as alloying elements to stabilize the high temperature hexagonal η-phase. However, the physical mechanism of this stabilization effect, especially on the high temperature η_1 and η_2 phases, is still unclear. In the present study, first-principle calculations were performed to study the stability and mechanical properties of Cu_5Sn_4 (η_1 and η_2) and Cu_6Sn_5 (η') when doped with Ni, Au, Zn, and indium alloying elements. It is shown that their phase stability and mechanical properties could be enhanced by these elements in some circumstances. Ni-doping can significantly enhance both the stability and the mechanical properties of the three phases, whereas Zn-doping exhibits a significant effect on that of the η_2 phase.

Key words: Intermetallic compounds, alloying effects, first-principle calculations, phase stability, mechanical properties

INTRODUCTION

Over the last few decades, Pb-free soldering alloy developments have been driven by legislative and environmental concerns. Among these solder alloys, Cu-Sn based solder alloys exhibit high strength and excellent weldability, which are commonly required in electronic and mechanical fields.[1,2] Generally, the solder joint is formed by the formation of interfacial intermetallic compounds (Cu_6Sn_5 in most cases) between solder and substrate. The phases that form in the solder interconnects, and their stability under service condition are crucial for the reliability of the final devices.[3] In numerous Sn-based solders, several intermetallic compounds (IMCs) may form during processing and cooling once copper reacts with tin-based alloys at high temperature in the Cu_6Sn_5 layer. Moreover, the formed IMCs layer can be as thin as 5 μm in thickness.[4,5] Thus, the mechanical reliability of the solder joints can be negatively affected by such excessive layer growth. Furthermore, the Cu_6Sn_5 phases not only have been used as solder alloys, but also have been proposed as an alternative electrode material for lithium ion batteries.[6,7] Hence, it is crucial to understand the structure-property relationship of the Cu_6Sn_5 phases for their applications in a wide range of industries.

The crystal structures of Cu_6Sn_5 are quite complex, and four Cu_6Sn_5 phases have been reported,

(Received September 29, 2015; accepted April 28, 2016; published online May 11, 2016)

which are η-Cu_6Sn_5, η_1-Cu_5Sn_4 (η^8), η_2-Cu_5Sn_4 (η^6) and η'-Cu_6Sn_5.[5,8–10] Recently, Wu et al.[11] also proposed a new structure named η^{4+1}, and this new monoclinic phase is constructed of four η_1 unit cells and one η' unit cell in a periodic stacking sequence. At equilibrium, the conventional unit cell of η'-Cu_6Sn_5 (space group C2/c, No. 15) has lattice parameters of a = 11.02 Å, b = 7.28 Å, c = 9.83 Å, and β = 98.84°.[8] However, the structure of the high temperature η-Cu_6Sn_5 phase has not been clearly understood due to its slight variations in composition and structure that occur with temperature change. In early 1973, the reported structure of η phase had the space group $P6_3/mmc$ (No. 194), and cell parameters of a = 4.192 Å and c = 5.037 Å.[10] In 1995, based on x-ray and electron diffraction results, Larsson et al.[9] proposed two structural models about η phase, i.e., η_1-Cu_5Sn_4 and η_2-Cu_5Sn_4, which are stable at high temperature. The η_1-phase, with the space group $P2_1/c$ (No. 14) and cell parameters of a = 9.83 Å, b = 7.27 Å, and β = 62.5°, was considered as stable at a temperature above 459 K, whereas the η_2-phase, with the space group C2 (No. 5) and cell parameters of a = 12.60 Å, b = 7.27 Å, c = 10.20 Å, and β = 90.0°, was believed stable at a temperature above 623 K.

Notably, the Cu_6Sn_5 IMCs demonstrate a phase transformation from hexagonal η-Cu_6Sn_5 to monoclinic η'-Cu_6Sn_5 when the temperature falls below ~462 K.[5,8–10] At room temperature (RT), the theoretical densities of the η and η' phases are 8.45 g/cm^3 and 8.27 g/cm^3, respectively. If the metastable η phase transforms into the stable η' phase at RT, the volume expansion is about 2%.[12,13] Under service conditions, such a volume change would produce a remarkable stress concentration and may cause failure of the solder interconnects. Therefore, it is a crucial issue to enhance the stability of Cu-Sn IMCs.

Several alloying elements (Ni, Au, Zn and indium) have been reported to have an effect on preventing the ~2% volume change associated with the hexagonal/monoclinic phase transformation.[14–19] Ni has a high solid solubility (~26 at.%) in the η-phase, and occupies the Cu sites to form $(Cu,Ni)_6Sn_5$. Ni-doping can inhibit the phase transformation.[14,15] Several experimental and theoretical investigations have been conducted to study the effects of Ni on the relative stability of the η and η' phases.[15–17]

Besides Ni, elements Zn, Au, and In, which all have good solubility in Cu_6Sn_5, have been investigated by Zeng et al.[17–19] It was found that these elements can also prevent the phase transformation. The experimental investigations indicated that Au can occupy the Cu site in Cu_6Sn_5, whereas Zn and indium may replace the Sn site. The first-principle calculations also predicted that the doped Zn can improve the stability of the low temperature η'-phase of Cu-Sn IMCs.[20,21] Recently, we also performed first-principle calculations to study the effects of alloying elements (Zn, indium, and Au) on the stability of the hexagonal η-phase,[18] which have been used as the reference results in this study. Nonetheless, the influence of the alloying elements on the stability of the high temperature monoclinic η_1 and η_2 phases of Cu_5Sn_4 with respect to the low temperature η'-phase of Cu_6Sn_5 still remains unclear. In the present study, we carried out extensive energy calculations to explore the phase stability and mechanical properties for the doped η', η_1 and η_2 phases of Cu-Sn IMCs, and our results provide physical insights about the mechanism of the stabilization effect of the alloying elements.

MODELS AND METHODS

Using Vienna *Ab initio* Simulation Package (VASP) code,[22,23] the reported structures of η'-Cu_6Sn_5, η_1-Cu_5Sn_4 and η_2-Cu_5Sn_4 were studied in detail for their relative stability and mechanical properties when doped with the alloying elements. The structure models of the three phases are provided in Fig. 1, drawn by the software VESTA.[24] The alloying elements, i.e., Ni, Au, Zn, and In atoms, were assumed to replace all Wyckoff sites of Cu(Sn) in the three IMCs to form different hypothetic structures, such that for each structure we can investigate its relative stability and mechanical properties in comparison with others. The projector augmented wave (PAW) method[25] was used to treat the interaction between ion and core electrons. The valence electrons for Cu($3d^{10}4s^1$), Ni($3d^8 4s^2$), Sn($5s^2 5p^2$), Au($5d^{10}6s^1$), Zn($3d^{10}4s^2$) and indium($5s^2 5p^1$) were described using the generalized gradient approximation (GGA) with the exchange–correlation functional of Perdew, Burke and Enzerhof (PBE).[26] Convergence tests indicated that 370 eV was a suitable cutoff energy for the PAW potential to obtain sufficient precision in the current systems. Brillouin-zone gridding was performed using the Monkhorst–Pack method[27] with 5 × 9 × 5 (η_1), 9 × 9 × 7 (η') and 3 × 5 × 3 (η_2) k-point meshes, which were sufficient for structural optimization. Nevertheless, finer k-meshes (11 × 11 × 9, 7 × 9 × 7, 5 × 7 × 5) were found to be better for calculating the relative formation enthalpies and mechanical properties. Using the optimal parameters, the calculated formation enthalpies change converge to better than 0.1 meV/atom.

To describe the stability of doped Cu-Sn IMCs with respect to the elemental solids (β-Sn, fcc-Cu), taking the $Cu_nSn_{m-x}X_x$ compound as an example, in which the alloying element X replaces the Sn-sites (X represents Ni, Au, Zn or indium). The formation enthalpy per atom (ΔH_f) and the relative formation enthalpy per atom (ΔH_{rf}) of a $Cu_nSn_{m-x}X_x$ IMC can then be defined as follows[28–30]:

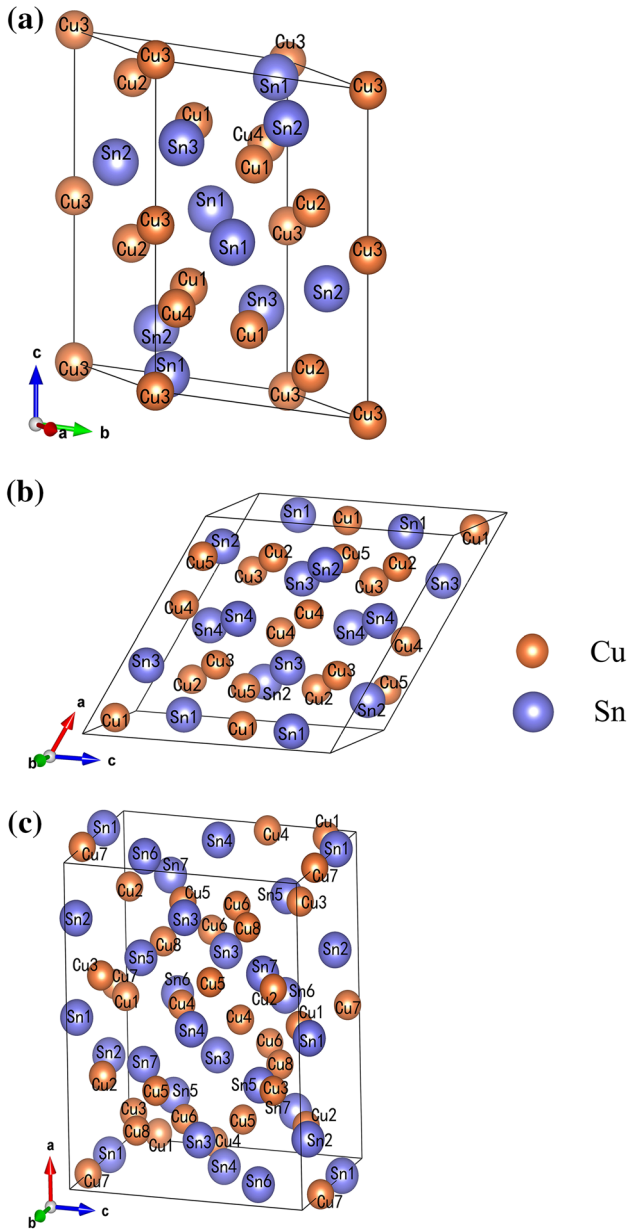

Fig. 1. Structures of three Cu-Sn IMCs with the Wyckoff positions denoted as numbers. (a) η'-Cu_6Sn_5, containing 12 Cu and 10 Sn atoms; (b) η_1-Cu_5Sn_4, containing 20 Cu and 16 Sn atoms; and (c) η_2-Cu_5Sn_4, containing 30 Cu and 24 Sn atoms.

$$\Delta H_f(\mathrm{Cu}_n\mathrm{Sn}_{m-x}X_x) = \frac{E(\mathrm{Cu}_n\mathrm{Sn}_{m-x}X_x) - [nE(\mathrm{Cu}) + (m-x)E(Sn) + xE(X)]}{m+n} \quad (1)$$

$$\Delta H_{rf} = \Delta H_f(Cu_nSn_{m-x}X_x) - \Delta H_f(Cu_nSn_m), \quad (2)$$

where $E(Cu_nSn_{m-x}X_x)$ is the total energy of a $Cu_nSn_{m-x}X_x$ phase; E(Cu), E(Sn) and $E(X)$ are energies of the pure elements Cu, Sn, and X per atom, respectively.

To further investigate how different elements affect the phase stability, the solution formation enthalpy $\Delta H_f^{atom}(X)$ of X atom can be defined as follow:

$$\Delta H_f^{atom}(X) = \frac{[E(Cu_nSn_{m-x}X_x) + xE_{Sn}^{bulk}] - [E(Cu_nSn_m) + xE_X^{atom}]}{x}, \quad (3)$$

where $E(\mathrm{Cu}_n\mathrm{Sn}_{m-x}X_x)$ and $E(\mathrm{Cu}_n\mathrm{Sn}_m)$ are the same as in Eq. 1. E_X^{bulk} is the bulk energy of each X atom; and E_X^{atom} is the single atom energy of X. E_X^{atom} can be calculated from a 12 Å × 12 Å × 12 Å cubic supercell with one X atom.

RESULTS AND DISCUSSION

Structural Parameters and Phase Stability

The alloying elements may replace different Wyckoff sites of Cu or Sn in the three Cu-Sn IMCs. To understand the crystallographic structures of doped Cu-Sn IMCs in relation to chemical bonding and mechanical properties, as well as the service performance of solder interconnects, it is necessary to identify their atomic structures for all fundamental phases involved.

Table I shows the calculated lattice parameters and binding energies for pure elements, which are comparable to previously reported results.[31] As known, tin has two allotropes, i.e., α-Sn and β-Sn. Since Cu-Sn IMCs form from the reaction between β-Sn and Cu, and β-Sn was observed to coexist with Cu_6Sn_5 in solder interconnects,[11,19] only the β-Sn structure is considered in our investigations.

Based on crystal structures shown in Table I, the formation enthalpies (ΔH_f) of η'-Cu_6Sn_5, η_1-Cu_5Sn_4 and η_2-Cu_5Sn_4 are calculated according to Eq. 1, and the results are listed in Table II. The differences in formation enthalpies among these phases are not very evident, while these data still clearly indicate the transformation sequence from η_2 to η_1 and then to η' upon cooling. We find that our formation enthalpy results for the η', η_1 and η_2 phases, which are −39.18 meV/atom, −35.19 meV/atom, and −32.51 meV/atom, are somewhat different in absolute value from that given in Ref. 3, where the three values are −33.21 meV/atom , −29.89 meV/atom, and −26.89 meV/atom. Nonetheless, the relative differences between these numbers are quite consistent in demonstrating the relative stabilities of the three phases. The difference between our results and the ones given in Ref. 3 is understandable, probably due to the different treatments for ion-electron and electron exchange-correlation interactions. Furthermore, our calculated lattice constants presented in Table II are in agreement with previously calculated results[3,32] and the experimental data.[9]

Table I. Calculated lattice constants and binding energies for the related metal elements

	Space group (No.)	Lattice constants (Å)	Energy (eV/atom)
Cu	$Fm\bar{3}m$ (225)	a = 3.631	−3.478
Ni	$Fm\bar{3}m$ (225)	a = 3.519	−4.838
Au	$Fm\bar{3}m$ (225)	a = 4.167	−2.983
Zn	$P6_3/mmc$ (194)	a = 2.656, c = 4.950	−1.101
In	I4/mmm (139)	a = 3.331, c = 4.966	−2.400
β-Sn	$I4_1/amd$ (141)	a = 5.934, c = 3.218	−3.166

Table II. Calculated formation enthalpies (meV/atom), lattice constants (in Å and degree), and Wyckoff atom sites for the three Cu-Sn IMCs using VASP calculations

	Lattice constants	Atom site	X Y Z (GGA)[a]	Experimental values[b]
η'-Cu_6Sn_5	a = 11.036[a], 11.119[b]	Cu1(8f)	0.103, 0.482, 0.205	0.101, 0.473, 0.202
C2/c	b = 7.288[a], 7.384[b]	Cu2(8f)	0.305, 0.505, 0.608	0.306, 0.504, 0.610
ΔH_f=−39.18	c = 9.841[a], 9.948[b]	Cu3(4a)	0.000, 0.000, 0.000	0.000, 0.000, 0.000
	β = 98.81[a], 98.73[b]	Cu4(4e)	0.000, 0.161, 0.250	0.000, 0.161, 0.250
		Sn1(8f)	0.389, 0.165, 0.531	0.391, 0.162, 0.529
		Sn2(8f)	0.290, 0.655, 0.361	0.285, 0.655, 0.358
		Sn3(4e)	0.000, 0.804, 0.250	0.000, 0.799, 0.250
η_1-Cu_5Sn_4	a = 9.830[a], 10.026[b]	Cu1(4e)	0.056, 0.776, 0.057	0.057, 0.779, 0.056
$P2_1c$	b = 7.270[a], 7.389[b]	Cu2(4e)	0.189, 0.256, 0.187	0.189, 0.253, 0.187
ΔH_f = −35.19	c = 9.830[a], 9.976[b]	Cu3(4e)	0.316, 0.725, 0.318	0.317, 0.725, 0.321
	β = 62.50[a], 61.96[b]	Cu4(4e)	0.430, 0.244, 0.431	0.427, 0.258, 0.427
		Cu5(4e)	0.191, 0.088, 0.938	0.188, 0.090, 0.937
		Sn1(4e)	0.071, 0.599, 0.285	0.071, 0.597, 0.287
		Sn2(4e)	0.183, 0.053, 0.436	0.180, 0.057, 0.440
		Sn3(4e)	0.324, 0.585, 0.578	0.313, 0.590, 0.583
		Sn4(4e)	0.456, 0.094, 0.668	0.451, 0.087, 0.663
η_2-Cu_5Sn_4	a = 12.600[a], 12.528[b]	Cu1(4c)	0.008, −0.022, 0.126	0.022, 0.007, 0.127
C2	b = 7.270[a], 7.511[b]	Cu2(4c)	0.335, 1.003, 0.126	0.343, 0.917, 0.129
ΔH_f=−32.51	c = 10.200[a], 10.463[b]	Cu3(4c)	0.661, 1.028, 0.128	0.653, 0.934, 0.133
	β = 90.00[a], 88.02[b]	Cu4(4c)	0.009, 0.003, 0.376	0.015, 0.030, 0.374
		Cu5(4c)	0.326, 0.996, 0.378	0.326, 0.999, 0.379
		Cu6(4c)	0.668, 0.023, 0.376	0.666, 0.036, 0.379
		Cu7(2a)	0.000, 0.656, 0.000	0.000, 0.692, 0.000
		Cu8(4c)	0.171, 0.846, 0.251	0.173, 0.853, 0.254
		Sn1(2a)	0.000, 0.303, 0.000	0.000, 0.333, 0.000
		Sn2(4c)	0.320, 0.349, 0.017	0.307, 0.349, 0.009
		Sn3(4c)	0.332, 0.339, 0.481	0.339, 0.352, 0.477
		Sn4(2b)	0.000, 0.336, 0.500	0.000, 0.360, 0.500
		Sn5(4c)	0.167, 0.201, 0.250	0.179, 0.210, 0.249
		Sn6(4c)	0.490, 0.159, 0.267	0.488, 0.190, 0.268
		Sn7(4c)	0.850, 0.160, 0.247	0.845, 0.164, 0.240

The corresponding experimental values are listed for comparison.[a]This study.[b]Ref. 9.

As seen in Fig. 1 and Table II, Cu atoms have four Wyckoff positions, while Sn atoms have three Wyckoff positions in the η'-Cu_6Sn_5 structure. We list the internal parameters of seven Wyckoff positions obtained from current calculations (at 0 K) in Table II, which are very close to the experimental measurements (at ambient temperature).[9] Similarly, the η_1-Cu_5Sn_4 structure has five(4) Wyckoff positions for Cu(Sn), while the η_2-Cu_5Sn_4 structure has eight (7) Wyckoff positions for Cu(Sn). The alloying elements Ni, Au, Zn and indium can occupy different Wyckoff positions of Cu or Sn to form hypothetic ternary $(Cu,Ni)_6Sn_5$, $(Cu,Au)_6Sn_5$, $(Cu,Zn)_6Sn_5$, $Cu_6(Sn,Zn)_5$ and $Cu_6(Sn,In)_5$ structures. For these doped structures, we can evaluate their relative formation enthalpies and mechanical properties using the first-principle calculations.

Figure 2 shows the relative formation enthalpies of all the hypothetic ternary structures formed by doping the fundamental binary η'-Cu_6Sn_5,

η_1-Cu_5Sn_4 and η_2-Cu_5Sn_4 structures at various sites with different alloying elements. The longitudinal coordinates are relative formation enthalpies plotted againgst hypothetic ternary structures corresponding to different Wyckoff atom sites in η' (Fig. 1a), η_1 (Fig. 1b), and η_2 (Fig. 1c) respectively. Each relative formation enthalpy value is obtained by subtracting the formation enthalpy of a fundamental binary structure from the calculated formation enthalpy of each hypothetic ternary structure,i.e., taking the three binary Cu-Sn IMCs (η',η_1, η_2) as three reference states (see Eq. (2)). When the alloying elements are doped, the phase stabilities of the three IMCs will change. The data show that the relative formation enthalpies can be significantly lowered when the Ni atoms occupy any Cu positions in all η'-Cu_6Sn_5, η_1-Cu_5Sn_4 and η_2-Cu_5Sn_4 structures. The formation enthalpies decrements are in the range of −40 meV/atom to −100 meV/atom, leading to enhanced thermodynamic stabilities for the three phases. Similar to Ni-doping, Au-doping may also enhance the phase stability when the Au atoms occupy most of the Cu positions in η'-Cu_6Sn_5, η_1-Cu_5Sn_4 and η_2-Cu_5Sn_4 structures, with the exception of the Cu4(4e) site in η', the Cu5(4e) site in η_1, and the Cu7(2a) and Cu8(4c) sites in η_2, as shown in Fig. 2a–c respectively. For Au-doping the formation enthalpies decrements are in the range of −20 meV/atom to −46 meV/atom and are smaller in magnitude than that of Ni.

Zn-doping and indium-doping, however, exhibit very different behaviors compared with Ni-doping and Au-doping. Firstly, Zn-doping has a negative effect on the phase stability of the Cu-Sn IMCs when Zn occupies all Cu-sites in the three IMCs, since the calculated relative formation enthalpies are all above the zeros in the three cases (Fig. 2a–c). Secondly, when Zn occupies the specific Sn6 sites to form the η_2-Cu_5Sn_3Zn structure (Fig. 2c), Zn-doping can stabilize the η_2-Cu_5Sn_4 phase by lowering its relative formation energy to −2.55 meV/atom. Thirdly, Zn-doping has no positive effect in stabilizing the η' and η_1 phases. Finally, indium-doping shows the most "smooth" variation in relative formation enthalpy, ranging from −4.78 meV/atom to +13.18 meV/atom. It can be seen that replacing the Sn-atoms at several positions in the η'-Cu_6Sn_5, η_1-Cu_5Sn_4 and η_2-Cu_5Sn_4 structures, indium-doping may enhance the phase stability of all the three phases. Moreover, indium-doping has obviously less stabilizing effect on the η'-phase as compared with its stabilizing effect on the η_1 and η_2 phases.

The specific positions with the lowest relative formation enthalpies of Cu-Sn IMCs doped with different elements are listed in Table III. As a result of the valence electron interaction between matrix elements (Cu, Sn) and doping atoms (Ni, Au, Zn or indium), the most energetic possible doped position will be different in each Cu-Sn IMC. It should be mentioned that in our calculations the Cu1 site is

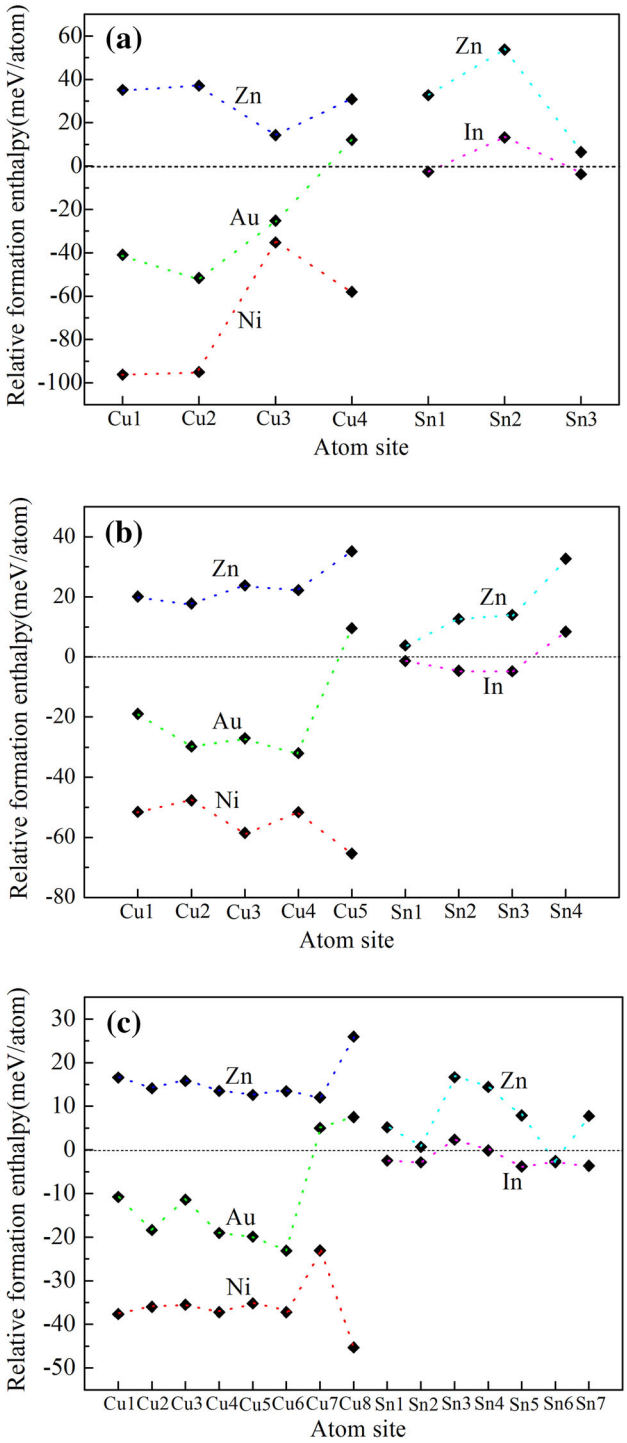

Fig. 2. Relative formation enthalpies (ΔH_{rf}) of doped η'-Cu_6Sn_5 (a), η_1-Cu_5Sn_4 (b) and η_2-Cu_5Sn_4 (c). Longitudinal coordinates are relative formation enthalpies, which are subtracted from the formation enthalpies of binary Cu_6Sn_5 IMCs (η', η_1, η_2). Horizontal coordinates are the Wyckoff atom sites in each IMC. Dashed lines are for guiding the eye.

energetically favorable for Ni substitution in η'-Cu_6Sn_5, which is different from Yu et al.,[16] who proposed that Ni atoms prefer to occupy the Cu2 site. By checking the relative formation enthalpies for Ni doping in the two positions, we found that

Table III. Lowest formation enthalpy positions with doped elements in IMCs

	Ni@Cu	Au@Cu	Zn@Cu	Zn@Sn	In@Sn
η'-Cu_6Sn_5	Cu1, 8f	Cu2, 8f	Cu3, 8f	Sn3, 4e	Sn3, 4e
η_1-Cu_5Sn_4	Cu5, 4e	Cu4, 4e	Cu2, 4e	Sn1, 4e	Sn3, 4e
η_2-Cu_5Sn_4	Cu8, 4c	Cu6, 4c	Cu7, 2a	Sn6, 4c	Sn5, 4c

Table IV. $\Delta H_f^{atom}(X)$ (eV/atom) of Ni and Zn in the lowest formation enthalpy positions

	Ni@Cu	Zn@Sn
η'-Cu_6Sn_5	−5.416	−1.030
η_1-Cu_5Sn_4	−5.475	−1.067
η_2-Cu_5Sn_4	−5.498	−1.135

they have nearly the same value. Both our results and other calculations[20] suggest that the Sn3 site is the most stable position for Zn substitution in η'-Cu_6Sn_5.

Based on Eq. 3 and Table III, one may further calculate the solution formation enthalpy $\Delta H_f^{atom}(X)$ for different alloying elements in the three phases. As examples, Table IV lists the calculated solution formation enthalpy values of Ni and Zn at the positions given in Table III. The results show that Ni and Zn atoms have lower solution formation enthalpy in a high temperature phase than in a low temperature phase, indicating that they can be doped a bit more easily in the η_1-Cu_5Sn_4 and η_2-Cu_5Sn_4 structures than in the η'-Cu_6Sn_5 structure.

It is important to further establish a correlation between our calculated results and the phase transformation from high temperature phase to low temperature phase. In experiments,[18,19] it was observed that when the alloying element content was increased up to $Cu_6Sn_{4.1}Zn_{0.9}$ or $Cu_6Sn_{4.1}In_{0.9}$ or $Cu_{5.1}Sn_5Au_{0.9}$, no peaks of the low temperature η'-phase appeared in powder x-ray diffraction (PXRD). Also, recent studies indicated that three alloy elements, i.e., Zn, Ni, and indium, can stabilize the high temperature hexagonal η-phase by forming $(Cu,Ni)_6Sn_5$, $Cu_6(Sn,Zn)_5$ and $Cu_6(Sn,In)_5$.[17–19] From our calculated data, the following points can be inferred about effects of the alloying element doping on the transformation from high temperature phase to low temperature phase. Firstly, about Zn-doping: (1) Zn-doping can stabilize the η_2-Cu_5Sn_4 phase by lowering its formation energy from −32.51 meV/atom to −35.06 meV/atom, and, therefore, may increase the energy barrier for the high temperature η_2-Cu_5Sn_3Zn to transform to the low temperature η'- Cu_5Sn_4 (with a formation energy of −39.18 meV/atom) without doping. (2) Furthermore, since Zn-doping shall increase the formation energy of η'-phase at least from −39.18 meV/atom to −32.82 meV/atom, the high temperature η_2-Cu_5Sn_3Zn (−35.06 meV/atom) cannot transform to the low temperature η'-Cu_6Sn_4Zn with doping. (3) Since the formation energy of Zn-doped η_1-Cu_5Sn_3Zn shall increase to −31.39 meV/atom, η_2-Cu_5Sn_3Zn would not transform to η_1-Cu_5Sn_3Zn, but η_1-Cu_5Sn_3Zn could transform to η'-Cu_6Sn_4Zn. Secondly, about indium-doping: indium-doping shows an effect similar to that of Zn-doping and could prevent the transformation from the high temperature η_2-Cu_5Sn_3In and η_1-Cu_5Sn_3In structures to the low temperature η'-Cu_6Sn_4In structure. Thirdly, about Ni-doping: (1) Ni-doping can stabilize the η_1 and η_2 phases by significantly lowering their formation energies and, therefore, may prevent the Ni-doped η_1-Cu_4NiSn_4 and the Ni-doped η_2-Cu_4NiSn_4 from their transformation to the η'-Cu_6Sn_5 without Ni-doping. (2) Nonetheless, since Ni-doping can also lower the formation energy of the η'-phase even more significantly by forming a η'-Cu_5NiSn_5 structure, the transformation from Ni-doped η_1-Cu_4NiSn_4 and η_2-Cu_4NiSn_4 to Ni-doped η'-Cu_5NiSn_5 would be still possible in terms of thermodynamic stability. Finally, about Au-doping: Au-doping shows an effect very similar to that of Ni-doping, and they differ only in magnitude of the effect.

From above results, it can be realized that in order to entirely explain the experimental observations about the transformation from high temperature phase to low temperature phase caused by alloying, not only formation energies of all possible phases need to be studied, but also more intensive experimental structure determination studies are needed to be conducted to precisely confirm which of all these hypothetic phases may form in reality.

Density of States

To further investigate how the stability of the three phases could be enhanced by alloying elements doping, the projected density states (PDOS) are plotted for Ni-and Zn-doped Cu-Sn IMCs, as shown in Fig. 3a–f, where only the most sable doped Cu-Sn structures are considered.

From the PDOS, it can be seen that the Zn's *d*-states have a tail towards the direction of the Fermi level due to the interaction between Zn-*d* and Sn-*s*/*p*, whereas the differences in the Zn-*d*'s shape and width can be negligible in the η', η_1 and η_2 phases. However, in Fig. 3f, we can observe a peak at the lower energy band edge of the Cu-*d* states and a few resonant peaks of the Zn-*s* states, especially those at −5 eV. In the energy range from −5 eV to +1 eV,

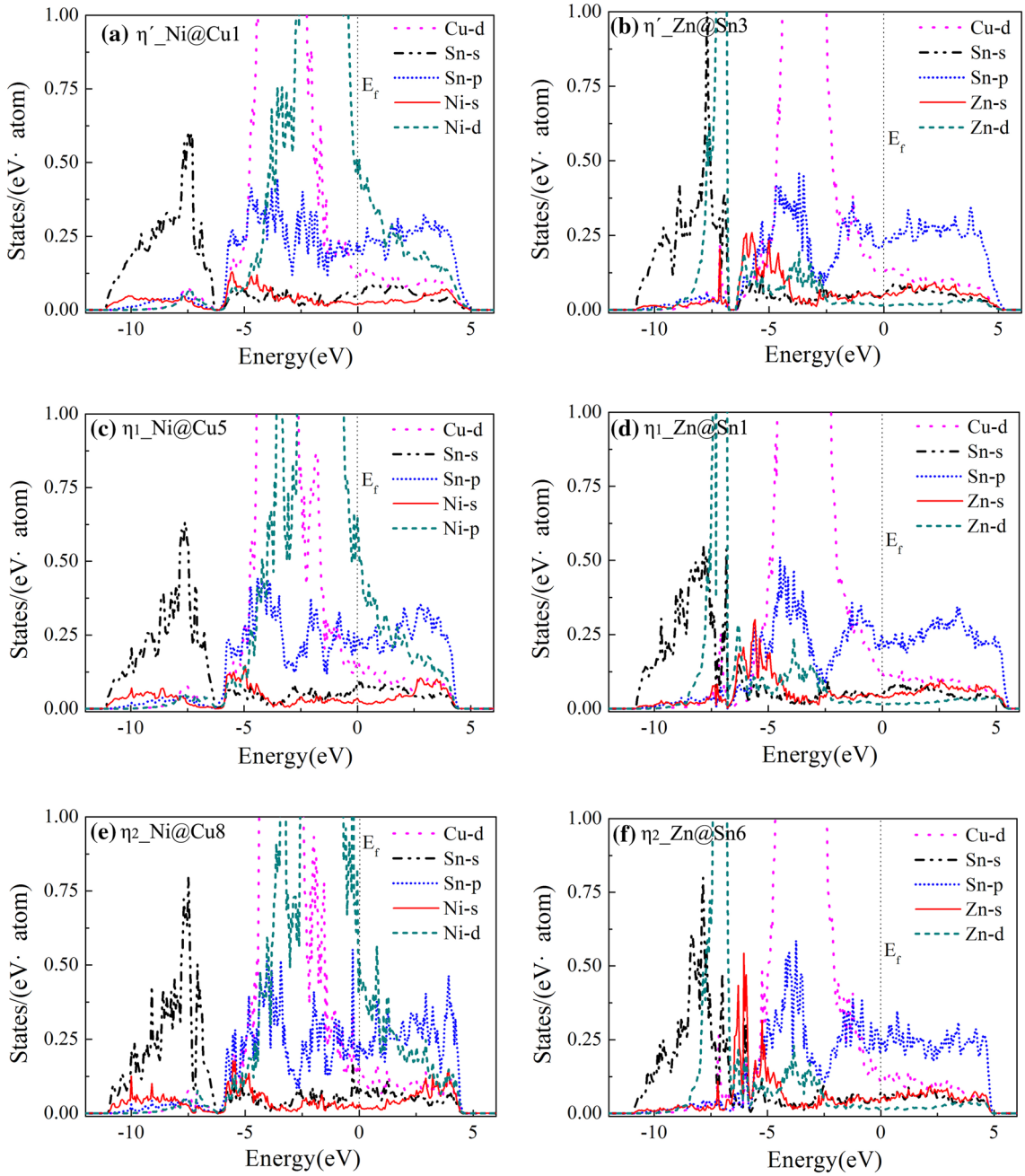

Fig. 3. Projected density of states (PDOS) of the doped Cu-Sn IMCs. (a) Ni doped η'-Cu_6Sn_5 at the Cu1 site; (b) Zn doped η'-Cu_6Sn_5 at the Sn3 site; (c) Ni doped η_1-Cu_5Sn_4 at the Cu5 site; (d) Zn doped η_1-Cu_5Sn_4 at the Sn_1 site; (e) Ni doped η_2-Cu_5Sn_4 at the Cu8 site; and (**f**) Zn doped η_2-Cu_5Sn_4 at the Sn6 site. The vertical dashed line E_f corresponds to the Fermi energy level.

Ni-*d* and Cu-*d* clearly overlap (see Fig. 3e), which results in a strong *d*–*d* interaction. Moreover, the width of Cu's *d*-band somewhat increases in the range of −5 eV to −2 eV in η_1 and η_2 with respect to that in η'. These electronic characters can cause a strong interaction between Zn-*s* and Cu-*d*. The unique orbital electron interaction between the alloying elements (Ni, Zn) and Cu should be the intrinsic reason that results in the enhanced stability of the three Zn(Ni) doped phases.

Mechanical Properties

For the Cu-Sn IMCs, the experimental elastic constants can in principle be obtained from nanoindentation or tensile testing. However, the experimental values may vary in scatter due to several factors such as sample preparation, anisotropic properties, or experimental methods. For example, the experimental Young's modulus of η'-Cu_6Sn_5 is in the range of 85-123 GPa.[3,32–34] Here, we performed

the first-principle calculations to evaluate the effects of doping elements on the mechanical properties of the doped Cu-Sn IMCs. Since several doping elements and doping sites are involved, over 20 IMCs need to be calculated. If using an ordinary procedure[28,30] to calculate the elastic constants of all the possible structures that actually have a very low symmetry, a huge amount of calculations would be required. To reduce computing time, we employed an equivalent but rapid computing method, the "universal linear-independent coupling strains" (ULICs) proposed by Yu et al.,[35] for the calculation of elastic constants.

As known, there are three independent elastic constants (C_{11}, C_{12} and C_{44}) for a cubic crystal, while a monoclinic crystal has ten more independent elastic constants, i.e., C_{13}, C_{15}, C_{22}, C_{23}, C_{25}, C_{33}, C_{35}, C_{46}, C_{55} and C_{66}. Among these elastic constants, C_{15}, C_{25}, C_{35} and C_{46} are extremely small (<5 MPa) for the IMCs, thus we ignored their contributions to the mechanical properties. Table V lists, for example, the calculated elastic constants for the doped η'-structures. It can be seen that the values shown in Table V are rather different and anisotropic. Ni and Zn increase the elastic constants, while Au and indium have almost no effect on these constants. The elastic constants are closed related to the substituting positions of the doped atoms. For instance, Zn at the Cu_3-site decreases the elastic constants, whereas Zn at the Sn_3-site has a positive effect on the constants. It should be noted that doping elements trend to increase the anisotropy of elastic constants in some structures. For instance, Au at the Cu_2-site decreases the elastic coefficients C_{ii} rather than C_{12}, C_{13}, and C_{23}. An increased anisotropy of elastic constants will enhance the mechanical properties, e.g., shear modulus.

Based on the Voigt approximation[36] and the elastic constants, a few crucial mechanical properties of the doped IMCs, such as bulk modulus (B), shear modulus (G), Young's modulus (E), and Poisson's ratio (υ), can be given as follows:

$$B = \frac{(C_{11} + C_{22} + C_{33})}{9} + \frac{2(C_{12} + C_{13} + C_{23})}{9}, \quad (4)$$

$$G = \frac{1}{15}(C_{11} + C_{22} + C_{33} - C_{12} - C_{13} - C_{23}) + \frac{1}{5}(C_{44} + C_{55} + C_{66}), \quad (5)$$

$$E = \frac{9BG}{3B + G}, \quad (6)$$

$$\upsilon = \frac{3B - 2G}{2(3B + G)}, \quad (7)$$

where B represents the ability to resist fracture; G represents the ability to resist plastic deformation, and a low (high) G/B value is related to the ductility (brittleness) of material.[37] Table VI lists the mechanical properties of all the doped structures in comparison with that of the three Cu-Sn IMCs and the hexagonal η-Cu_6Sn_5 phase in addition. The purpose for re-calculating the values for the previously investigated hexagonal η-Cu_6Sn_5 phase and its doped structures is to demonstrate that our calculation results can be in good agreement with the following experimental measurement: Zn-doping not only stabilizes the η-Cu_6Sn_5 phase,[18] but also can increase the Young's modulus by about 10 GPa, which was obtained from both a nanoindentation measurement[38] and our calculation, though only the relative or difference values, not the absolute values, are in agreement. It is noticeable that our calculated values are lower than the experimental data by about 40 GPa. Nonetheless, the ULICs method can still be used to estimate the mechanical properties of the Cu-Sn IMCs under the present investigation.

Table VI clearly shows that Ni and Zn can enhance the mechanical properties of the η', η_1 and η_2 phases. For the η'-Cu_6Sn_5 phase, the bulk modulus (B), shear modulus (G), and Young's modulus (E) can be increased with Ni-doping by 17%, 32%, and 30%, respectively, though the Poisson's ratio (υ) may decrease by 6%. Similar positive changes can be found for the η_1 and η_2 phases. (see Table VI). Since Ni is a strong stabilizer for all the Cu-Sn IMCs (Fig. 2), due to the strong Sn-p and Ni-d interaction (Fig. 3), the mechanical reliability of integrated circuits during a thermal cycle can be enhanced in any way by Ni-doping. Although Zn is

Table V. Calculated elastic constants (GPa) for η'-Cu_6Sn_5 and doped η'-Cu_6Sn_5

	C_{11}	C_{22}	C_{33}	C_{44}	C_{55}	C_{66}	C_{12}	C_{13}	C_{23}
η'-Cu_6Sn_5	129.10	131.94	118.74	34.84	17.52	35.38	49.50	54.88	55.21
$(Cu,Ni)_6Sn_5$-Ni@Cu1	157.39	159.80	154.16	47.20	24.78	41.09	55.08	56.41	61.43
$(Cu,Au)_6Sn_5$-Au@Cu2	122.58	121.27	115.26	27.39	12.99	31.31	56.94	56.41	56.18
$(Cu,Zn)_6Sn_5$-Zn@Cu3	120.11	118.63	110.98	29.89	14.64	26.33	53.32	48.82	52.96
$Cu_6(Sn,In)_5$-In@Sn3	129.36	129.65	121.67	36.28	20.67	37.29	48.70	55.57	59.65
$Cu_6(Sn,Zn)_5$-Zn@Sn3	137.81	138.97	129.85	39.55	20.19	36.34	46.93	53.12	57.91

Table VI. Calculated mechanical properties of the Cu-Sn IMCs and the doped Cu-Sn IMCs

	Doping concentration (at.%)	B (GPa)	G (GPa)	G/B	E (GPa)	ν
η'-Cu_6Sn_5	–	77.66	32.23	0.42	84.93	0.318
		79.6[a], 80.9[b]	35.9[a]	0.45[a]	85[c]	0.31[a]
$(Cu,Ni)_6Sn_5$-Ni@Cu1	18.2	90.80	42.51	0.47	110.31	0.298
$(Cu,Au)_6Sn_5$-Au@Cu2	18.2	77.57	26.98	0.35	72.52	0.344
$(Cu,Zn)_6Sn_5$-Zn@Cu3	9.1	73.32	27.15	0.37	72.49	0.335
$Cu_6(Sn,Zn)_5$-Zn@Sn3	9.1	80.28	35.79	0.45	93.49	0.306
$Cu_6(Sn,In)_5$-In@Sn3	9.1	78.72	33.30	0.42	87.55	0.315
η_1-Cu_5Sn_4	–	79.39	32.37	0.41	85.48	0.321
		81.7[a], 81.7[b]				
$(Cu,Ni)_5Sn_4$-Ni@Cu5	11.1	85.58	37.83	0.44	98.91	0.307
$(Cu,Au)_5Sn_4$-Au@Cu4	11.1	77.54	25.81	0.33	69.69	0.350
$Cu_5(Sn,Zn)_4$-Zn@Sn1	11.1	83.00	34.56	0.42	91.04	0.317
$Cu_5(Sn,In)_4$-In@Sn3	11.1	78.59	30.27	0.39	80.48	0.329
η_2-Cu_5Sn_4	–	78.01	27.33	0.35	73.41	0.343
		81.5[a], 81.1[b]				
$(Cu,Ni)_5Sn_4$-Ni@Cu8	7.4	81.92	32.97	0.40	87.21	0.323
$(Cu,Au)_5Sn_4$-Au@Cu6	7.4	77.99	28.57	0.37	76.39	0.337
$Cu_5(Sn,Zn)_4$-Zn@Sn6	7.4	82.04	39.23	0.49	101.51	0.294
$Cu_5(Sn,In)_4$-In@Sn5	7.4	78.25	31.31	0.40	82.88	0.323
η-Cu_6Sn_5	–	75.01	30.74	0.41	81.14	0.320
					119.7±3[d]	
$(Cu,Ni)_6Sn_5$-Ni@Cu1	4.5	79.79	32.87	0.38	86.70	0.319
$(Cu,Au)_6Sn_5$-Au@Cu3	4.5	76.71	29.78	0.39	79.10	0.328
$Cu_6(Sn,Zn)_5$-Zn@Sn2	4.5	79.89	35.29	0.44	92.28	0.307
					127.8±5[d]	
$Cu_6(Sn,Zn)_5$-In@Sn2	4.5	77.55	32.43	0.42	85.39	0.316

[a]Calculated results from Ref. 3.[b]Calculated results from Ref. 32.[c]Experimental results from Ref. 34.[d]NIT results from Ref. 38.

not a strong stabilizer in the three Cu-Sn IMCs as compared with Ni, some mechanical properties, for example, the Young's modulus and shear modulus of the Zn-doped η_2-Cu_6Sn_5 phase can increase significantly by 38.3% and 43.5%, respectively, mostly due to its increased anisotropy between diagonal and off-diagonal elements in the elastic coefficient matrix (as mentioned in the discussion about Table V): its diagonal elements are increased by numbers up to ~26 GPa, whereas off-diagonal elements are decreased by numbers down to 9 GPa in the η_2-$Cu_5(Sn,Zn)_4$-Zn@Sn6 phase in comparison with that for η_2-Cu_5Sn_4. As compared with Ni and Zn, Au-doping and indium-doping have small influences on the mechanical properties of the Cu-Sn IMCs.

To demonstrate the brittleness (ductility) of the doped Cu-Sn IMCs, the Cauchy pressures, i.e., (C_{12}–C_{44}), are plotted against the Pugh's modulus ratios for selected doped Cu-Sn structures, as shown in Fig. 4. If the following two criterions hold: its Pugh's modulus ratio G/B[37] is less than 0.57 and its Cauchy pressure[39] is positive, the material will appear to have metallic bonding. Otherwise it will be covalent bonding. The higher the (C_{12}–C_{44}) value and the lower the G/B value, the more ductile the material is. Previous studies[40,41] have demonstrated the validity of the above two criteria in studying the ductile-brittle transition in the IMCs. Figure 4 clearly demonstrates that Cauchy pressures for all the selected Cu-Sn IMCs (with or without doping elements) are positive and their Pugh's ratios are all smaller than 0.57, indicating all these structures are metallic and ductile. The alloying element doping has no remarkable effect on the ductility of

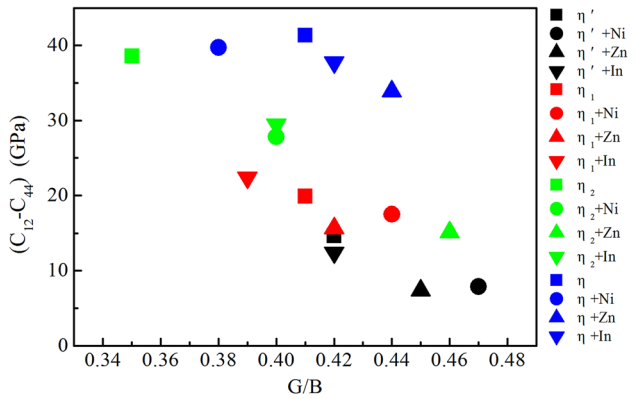

Fig. 4. Correlation between the Cauchy pressure (C_{12}–C_{44}) and the Pugh's modulus ratio G/B for the doped η', η_1, η_2 and η phases. The lowest enthalpy doping positions in Table III were selected. Black symbols denote η'-Cu_6Sn_5 and doped η'-Cu_6Sn_5; red symbols denote η_1-Cu_5Sn_4 and doped η_1-Cu_5Sn_4; green symbols denote η_2-Cu_5Sn_4 and doped η_2-Cu_5Sn_4 doped η_1-Cu_5Sn_4; and blue symbols denote η-Cu_6Sn_5 and doped η-Cu_6Sn_5 (Color figure online).

the three Cu-Sn IMCs under the present investigation.

CONCLUSION

The doping effects of Ni, Au, Zn, and indium on the phase stability and the mechanical properties of the η'-Cu_6Sn_5, η_1-Cu_5Sn_4 and η_2-Cu_5Sn_4 phases among Cu-Sn IMCs have been systematically investigated using DFT calculations. From the present study, the following conclusions are obtained:

1. Ni-doping can stabilize the η',η_1 and η_2 phases by significantly lowering their formation energies and can significantly increase their mechanical properties. Nonetheless, since Ni-doping can lower the formation energy of the η'-phase even more significantly, the transformation from Ni-doped η_1-Cu_4NiSn_4 and η_2-Cu_4NiSn_4 to Ni-doped η'-Cu_5NiSn_5 would be still possible. Au-doping shows an effect on the stability of the three phases in a way similar to Ni-doping, but has a very small effect on their mechanical properties.
2. At the specific Sn_6 positions in the η_2-phase, Zn can stabilize the η_2-structure and significantly increase its Young's modulus and shear modulus. Since Zn cannot stabilize the η' and η_1 phases, the transformation from the doped η_2-phase to both the doped η' and η_1 phases could be prevented. Similarly, occupying some specific Sn positions in the three phases, indium-doping can stabilize these phases to different extents and would prevent the transformation from the doped high temperature η_1 and η_2 phases to the doped low temperature η' phase. Nonetheless, indium has a small influence on the mechanical properties of the three phases.

ACKNOWLEDGEMENTS

This work is supported by the National Natural Science Foundation of China (Nos. 11427806, 51471067, 51371081, 51171063), the National Basic Research (973) Program of China (No. 2009CB623704), and Hunan Provincial Natural Science Foundation of China (No. 14JJ4052). The author thanks Dr. Kazuhiro Nogita from the University of Queensland for his valuable input on the early stage of this project.

REFERENCES

1. F. Kohler, T. Campanella, S. Nakanishi, and M. Rappaz, *Acta Mater.* 56, 1519 (2008).
2. K. Nogita, C.M. Gourlay, S.D. McDonald, Y.Q. Wu, J. Read, and Q.F. Gu, *Scr. Mater.* 65, 922 (2011).
3. G. Ghosh and M. Asta, *J. Mater. Res.* 20, 3102 (2005).
4. T. Laurila, V. Vuorinen, and J.K. Kivilahti, *Mat. Sci. Eng. R* 49, 1 (2005).
5. N. Saunders and A.P. Miodownik, *Bull. Alloy Phase Diagrams* 11, 278 (1990).
6. S.H. Ju, H.C. Jang, and Y.C. Kang, *J. Power Sources* 189, 163 (2009).
7. K.D. Kepler, J.T. Vaughey, and M.M. Thackeray, *Electrochem. Solid-State Lett.* 2, 307 (1999).
8. A.K. Larsson, L. Stenberg, and S. Lidin, *Acta Crystallogr. Sect. B* 50, 636 (1994).
9. S. Lidin and A.K. Larsson, *J. Solid State Chem.* 118, 313 (1995).
10. A.K. Larsson, L. Stenberg, and S. Lidin, *Z. Kristallogr.* 210, 832 (1995).
11. Y.Q. Wu, J.C. Barry, T. Yamamoto, Q.F. Gu, S.D. McDonald, S. Matsumura, and K. Nogita, *Acta Mater.* 60, 6581 (2012).
12. C.Y. Chou and S.W. Chen, *Acta Mater.* 54, 2393 (2006).
13. K. Nogita, C.M. Gourlay, and T. Nishimura, *JOM* 61, 45 (2009).
14. U. Schwingenschlogl, C. Di Paola, K. Nogita, and C.M. Gourlay, *Appl. Phys. Lett.* 96, 061908 (2010).
15. K. Nogita, D. Mu, S.D. McDonald, J. Read, and Y.Q. Wu, *Intermetallics* 26, 78 (2012).
16. C. Yu, J. Liu, H. Lu, P.L. Li, and J.M. Chen, *Intermetallics* 15, 1471 (2007).
17. G. Zeng, S.D. McDonald, Q. Gu, Y. Terada, K. Uesugi, H. Yasuda, and K. Nogita, *Acta Mater.* 83, 357 (2015).
18. G. Zeng, S.D. McDonald, Q. Gu, S. Suenaga, Y. Zhang, J.H. Chen, and K. Nogita, *Intermetallics* 43, 85 (2013).
19. G. Zeng, S.D. McDonald, Q. Gu, and K. Nogita, *J. Mater. Res.* 27, 2609 (2012).
20. Y. Yang, Y. Li, H. Lu, C. Yu, and J.M. Chen, *Comp. Mater. Sci.* 65, 490 (2012).
21. W.Q. Shao, C.Y. Yu, W.C. Lu, J.G. Duh, and S.O. Chen, *Mater. Lett.* 93, 300 (2013).
22. G. Kresse and J. Furthmüller, *Phys. Rev. B* 54, 11169 (1996).
23. G. Kresse and J. Furthmüller, *Comp. Mater. Sci.* 6, 15 (1996).
24. K. Momma and F. Izumi, *J. Appl. Crystallogr.* 44, 1272 (2011).
25. G. Kresse and D. Joubert, *Phys. Rev. B* 59, 1758 (1999).
26. J.P. Perdew, K. Burke, and M. Ernzerhof, *Phys. Rev. Lett.* 77, 3865 (1996).
27. H.J. Monkhorst and J.D. Pack, *Phys. Rev. B* 13, 5188 (1976).
28. Z.R. Liu, J.H. Chen, S.B. Wang, D.W. Yuan, M.J. Yin, and C.L. Wu, *Acta Mater.* 59, 7396 (2011).
29. S.B. Wang, J.H. Chen, M.J. Yin, Z.R. Liu, D.W. Yuan, J.Z. Liu, C.H. Liu, and C.L. Wu, *Acta Mater.* 60, 6573 (2012).
30. L.H. Liu, J.H. Chen, T.W. Fan, Z.R. Liu, Y. Zhang, and D.W. Yuan, *Comp. Mater. Sci.* 108, 136 (2015).
31. J. Klimeš, D.R. Bowler, and A. Michaelides, *Phys. Rev. B* 83, 195131 (2011).
32. S. Ramos de Debiaggi, C. Deluque, G. Toro, F. Cabeza, and A. Fernández Guillermet, *J. Alloys Compd.* 542, 280 (2012).
33. G.Y. Jang, J.W. Lee, and J.G. Duh, *J. Electron. Mater.* 33, 1103 (2004).
34. B. Subrahmanyam, *Trans. Japan Inst. Metals* 13, 93 (1972).
35. R. Yu, J. Zhu, and H.Q. Ye, *Comput. Phys. Commun.* 181, 671 (2010).
36. R. Hill, *Proc. Phys. Soc. A* 65, 349 (1952).
37. S.F. Pugh, *Philos. Mag.* 45, 823 (1954).
38. S.X. Chen, W. Zhou, and P. Wu, *J. Electron. Mater.* 44, 3920 (2015).
39. D.G. Pettifor, *Mater. Sci. Technol.* 8, 345 (1992).
40. K. Chen, L.R. Zhao, and J.S. Tse, *J. Appl. Phys.* 93, 2414 (2003).
41. H. Wang, Z.D. Zhang, R.Q. Wu, and L.Z. Sun, *Acta Mater.* 61, 2919 (2013).